Surface & Coatings Technology 258 (2014) 566–573

Contents lists available at ScienceDirect

Surface & Coatings Technology

journal homepage: www.elsevier.com/locate/surfcoat

Microstructure and wear properties of AISI M2 tool steel on RF plasma nitriding at different N_2–H_2 gas compositions

R. Mohammadzadeh [a], A. Akbari [a,*], M. Drouet [b]

[a] Faculty of Materials Engineering, Sahand University of Technology, P. O. Box 51335-1996, Tabriz, Iran
[b] Institut PPRIME, UPR 3346, University of Poitiers, CNRS, ENSMA, Dpt. of Physics and Mechanics of Materials, F-86962 Futurocope Cedex, France

ARTICLE INFO

Article history:
Received 27 April 2014
Accepted in revised form 16 August 2014
Available online 23 August 2014

Keywords:
Plasma nitriding
Wear resistance
M2 tool steel
Gas composition
Microhardness
Nitrided layer depth

ABSTRACT

Wear behavior of quenched-tempered AISI M2 tool steel samples has been studied after plasma nitriding at different N_2–H_2 plasma gas flows containing 25, 50 and 75 sccm N_2. Plasma nitriding was performed at 450 °C for 8 h under floating potential using a plasma reactor equipped with a radio frequency power generator. Microstructure, phase composition, nitrided layer thickness, hardness and surface roughness of the samples were studied using optical microscopy, X-ray diffraction, microhardness and surface profilometry measurements. Dry sliding wear resistance of samples was determined by performing ball-on-disc wear testes. The results revealed formation of mainly a diffusion zone at the 25 sccm N_2–75 sccm H_2 gas flow and mono-phase ε-$Fe_{2-3}N$ compound layer at higher N_2 concentrations. Plasma nitriding increases near surface hardness up to 50% (about $1600HV_{0.025}$) irrespective of the N_2:H_2 ratio, where nitrided layer depth and surface roughness increase with increasing the N_2 flow rate in the plasma gas. Depending on the nitrogen content, sliding wear resistance may be improved between 20 and 90% with respect to the un-nitrided substrate. Among the nitrided samples the maximum and minimum wear resistance was obtained at plasma gases containing higher and lower H_2 fractions, respectively. Decreasing wear resistance with increasing N_2 flow rate in the plasma gas attributed to formation of the hard and brittle compound (white) layer on the sample surface and development of residual stress profiles.

1. Introduction

AISI M2 high speed tool steel is a widely used material to manufacture cutting tools. The cutting tools have quite complex geometries and normally are made from high-cost materials. The most commonly occurring problems associated with these materials are wearing of the cutting edge and adhesion of the work material to the tool [1–3]. Tribological problems can often be solved by an appropriate surface modification technique. Plasma nitriding, owing to a number of advantages over the conventional gas and salt bath nitriding processes, has found increasing industrial applications [4]. The salt bath nitriding poses major problems related to toxicity of the cyanid–cyanat salts. The conventional gas nitriding requires longer process times to get the desired nitrided case depths [5,6].

Direct current plasma nitriding (DCPN) is one of the conventional plasma assisted surface engineering processes widely used in the industry to improve the mechanical properties and wear resistance of engineering materials over the past years [7]. However, The DCPN technology suffers from some serious technological and inherent shortcomings which limit its further development. The technological limitations with respect to the conventional nitriding processes are related to the higher equipment costs and the lack of thorough understanding of the process. The intrinsic problems are related to the mode of plasma generation in which the components are subjected to high cathodic potentials. There are difficulties in maintaining a uniform temperature inside the plasma chamber [8]. On the other hand, the components to be treated are subjected to "arcing" [7], "edge effects" [9,10], and "hollow cathode effect" [11].

In order to eliminate the common problems associated with the DCPN and enhance nitriding efficiency, different plasma techniques have been developed such as; pulsed dc plasma nitriding, plasma immersion ion implantation and radio frequency (RF) plasma nitriding, which have been successfully scaled up at industrial scale [12–14]. Recently, an active screen plasma nitriding (ASPN) system also exhibited some advantages over the DCPN in laboratory scale, despite providing lower plasma intensity and prolonging nitriding time [7–11]. A system with RF plasma has some important advantages over the other plasma sources that provide motivation for study of the RF plasma nitriding. For example, gas pressure can be much lower in RF plasma (0.2–10 Pa) than in DC plasma (100–1000 Pa), leading to lower consumption of feed gas [12,13]. Also, plasma generation is separated from the substrate bias, hence removing the need for arc suppression and allowing

* Corresponding author. Tel.: +98 411 3459416; fax: +98 411 3444333.
E-mail address: akbari@sut.ac.ir (A. Akbari).

http://dx.doi.org/10.1016/j.surfcoat.2014.08.036
0257-8972/

better control of the process [12–14]. Thus, insulating and electrically resistant materials can be more successfully nitrided using RF plasma [12]. On the other hand, the nitriding time is shorter and the nitride layer thickness falls more slowly with lowering temperature than with other plasma nitriding environments.

As a result of plasma nitriding, different zones may form at the component surface, known as the compound layer(s) and diffusion zone from surface to core, respectively. Depending on the steel composition, the compound layer is composed mainly of iron nitrides (γ'-Fe_4N and/or ε-$Fe_{2-3}N$) and nitrides of alloying elements as well. The layer beneath the compound layer(s), known as the so called "diffusion zone", consists mainly of a solid solution of interstitial nitrogen atoms in the iron and nitride precipitates [4–6].

Research studies have shown that the microstructure of the nitrided layer can be affected by changing process parameters such as temperature, time and plasma gas composition. The changes in the microstructure of the nitrided layer affects the mechanical and tribological properties of the material such as surface hardness wear resistance and fatigue limit [5,15]. As expected for diffusion controlled growth, nitrided layer thickness and hence cross-sectional hardness profile increase with increasing nitriding temperature and time; however, the maximum surface hardness is achieved at a particular nitriding time and temperature [15–17].

Efficient plasma nitriding of an alloy requires higher density of the reactive nitrogen species such as molecular ions (N_2^+), exited molecules (N_2^*), ions N^+ and radicals (N) [18]. Mixing hydrogen with nitrogen enhances reactive nitrogen species due to the fact that the dissociation (8.8 eV) and ionization (13.1 eV) energies of the H_2 gas are smaller than the dissociation (24 eV) and ionization energies (15.58 eV) of the N_2 gas [19]. Therefore, in plasma nitriding of metals and alloys mixtures of N_2–H_2 instead of N_2 are used as plasma gas [19–21]. The beneficial effects of H_2 in the N_2–H_2 plasma take place through the following distinct effects: (i) removing (reduction) initial oxide layer from the sample surface and chemical etching of the oxygen during nitriding [18–20], and (ii) increasing the density of reactive nitrogen species in the plasma and the nitrogen chemical potential on the component surface [19–21]. Priest et al. [21] conducted RF plasma nitriding of AISI 316 austenitic stainless steel with N_2, N_2–H_2 plasma gases with and without H_2 pre-cleaning prior plasma nitriding. They concluded that greater nitrided layer thickness obtained using N_2–H_2 gas mixture than pre-cleaning with H_2 prior RF plasma nitriding in pure N_2 indicates an additional effect of H_2 beneath the surface of the substrate (~μm).

Previous studies have indicated the importance of the nitrogen chemical potential in plasma nitriding of steels. However, there has not been a systematic detailed study on the relation between the RF plasma gas composition, microstructure and mechanical properties. The aim of the present paper is studying the RF plasma nitriding behavior of quenched-tempered AISI M2 steel at different N_2–H_2 gas mixtures. The changes in compound layer formation; nitrided layer depth, hardness, and wear resistance are investigated using X-ray diffraction, optical microscopy, microhardness tests, ball on disc wear tester, and 3D surface profilometry.

2. Experimental

Cylindrical samples with 32 mm diameter and 8 mm thick were cut from AISI M2 high speed tool steel bar with chemical composition of Fe–0.819C–5.71W–5.27Mo–3.88Cr–1.13V–0.101Co–0.260Mn in wt.%. The elemental composition was obtained by optical emission spectroscopy analysis using a SpectroLab M5 analyzer. The steel bar in the as-received condition has a hot deformed structure, with a hardness of 28 HRC. Before plasma-nitriding treatment, all of the samples were subjected to a heat treatment cycle to achieve hardened-tempered state with a core hardness of 65 ± 1 HRC (850 HV_{30}–1040 $HV_{0.025}$) in order to provide sufficient load carrying capacity. The quench-tempering heat treatment cycle was performed in a molten salt bath according to DIN17350 standard [22] as follows:

- Preheating: at 450 °C for 30 min and then at 850 °C for 5 min
- Austenitizing: at 1205 °C for 2 min
- Quenching: in salt bath (up to 510 °C) and then cooling in air
- Tempering: three times at 555 °C for 80 min

After quench-tempering heat treatment and before nitriding, samples were polished carefully with SiC abrasive papers 80 to 1500 (European FEPA or P-Grading) followed by mirror polishing using 1 μm diamond paste until the surface roughness, R_a values, reached the range of 20–40 nm. Finally, all samples were ultrasonically cleaned successively in acetone and ethanol then dried under a nitrogen flow before plasma nitriding.

Samples were plasma nitrided using the URANOS plasma reactor operating under floating potential conditions [23,24]. Further details of the URANOS reactor have been explained elsewhere [25]. Plasma was generated using a 100 sccm N_2–H_2 plasma gas flow containing different flows (gas mixtures) of 25 sccm N_2–75 sccm H_2; 50 sccm N_2–50 sccm H_2; and 75 sccm N_2–25 sccm H_2 in a quartz tube by means of a 13.56 MHz RF power source operating at 750 W working power. For the sake of simplicity, in the following, the above plasma gas flows are denoted with $25N_2$, $50N_2$ and $75N_2$, respectively. The process temperature and working pressure were 450 °C and 7.5 Pa, respectively. Process temperature was chosen to be about 100 °C below the tempering temperature of the AISI M2 steel. In this reactor heating is provided by an external electrical furnace which enables the process temperature to be controlled independently from the plasma. During the process no sputtering is produced. Active species that reach sample surface produce adsorption, dissociation and then diffusion; the quality of the sample surface is determinant for the nitrogen transfer to the solid. To avoid undetermined surface effects and maintain reproducibility, a systematic surface preparation protocol was used as described above. After nitriding for 8 h, the samples were allowed to cool in the vacuum chamber but outside the furnace where the temperature reached less than 200 °C after 15 min.

The phase composition of un-nitrided and nitrided substrates was studied by means of X-ray diffraction (XRD) using a Bruker D8 advanced diffractometer with monochromatic Cu-K_α radiation ($\lambda = 1.5406$ Å) in the Bragg–Brentano configuration operated at 40 KeV and 40 mA. XRD diffraction patterns were recorded with a step size of 0.02° and a step duration of 4 s at each step in the angular range of 10°–130°. The microstructure of transverse sections of the un-nitrided and nitrided samples was studied using an Olympus-PMG3 optical microscope.

Surface and cross-sectional hardness of the samples were investigated using MDPEL-M400 GL microhardness tester equipped with a Vickers indenter. Measurements were performed under the load of 0.245 N (25 g) applied for 15 s on the mechanically polished and cleaned surfaces. Microhardness profiles were obtained from the average of four measurements, taken from four distinct regions of the cross-section at a given depth. Nitrided case depth was determined according to the JIS G0562 standard [26] by measuring distance from the surface to the point that its hardness was about 50 HV higher than the hardness of un-nitrided substrate.

The surface roughness of the as-polished and as-nitrided specimens was measured using a Mitutoyo Surftest SJ-301 profilometer.

Sliding wear tests were carried out using a ball-on-disc wear tester, according to ASTM G 99-95a [27] standard procedure. During tests, AISI M2 tool steel discs rotated against a stationary sapphire ball of 5 mm in diameter at the speed of 30 rpm. Wear tests were performed under a constant load of 8 N and at a sliding distance of 1000 m and a wear track diameter of 12 mm. All tests were performed at room temperature and un-lubricated condition in laboratory air. Wear tracks were characterized using a Talysurf CCI 6000 3D optical profiler [28] in order to digitize the wear track profile. Removed material volume was obtained from analysis of the 3D surface profiles of the wear tracks using the

Mountains Map Universal software 4.1 [29]. Generally the wear track of relatively ductile materials contains a hole at the center and a piled up regions at the lateral sides of the track. The creation of piled up regions takes place via the aside material displacement due to plastic deformation of the disc material. The surface area of the wear hole and the pile-up volume were extracted from the averaged line profile. The net worn out material volume, V_w was then calculated using the following equation:

$$V_w = V_r\text{-}V_p = \left(S_r - S_p\right) \times L \quad (1)$$

where V_r and S_r are the removed material volume and surface, respectively, V_p and S_p are the material volume and surface in pile up, respectively, and L is the scanned track length in profilometry.

3. Results

3.1. Optical microstructures

Representative optical micrographs taken from polished and etched cross-section of samples nitrided at three different plasma gas compositions are shown in Fig. 1. This figure indicates also the microstructure of the substrate prior to nitriding. In the quenched and triple tempered condition the microstructure of M2 tool steel consisted of the well known tempered martensite with dispersed primary and secondary alloy carbides. The nitrided layer appears as a dark zone at the top of micrographs. The compound (white) layer could not be distinguished from the optical microscopy images. In fact the microstructure of the diffusion zone is almost identical to that of the substrate core, but it is darker than the core, where the nitrogen is found in a solid solution or nitrides of alloying elements. It is seen from optical microscopy images (Fig. 1) that the thickness of the diffusion zone increases with increasing the amount of the nitrogen content in the plasma gas flow up to 50 sccm. The thickness of the diffusion zone did not increase considerably by further increasing of the N_2 content, i.e. at the 75 sccm nitrogen, in the plasma gas flow.

3.2. Microhardness profiles

Cross sectional microhardness depth profile of samples nitrided under different plasma gas composition (flow rate) is illustrated in Fig. 2. The results clearly show that the near surface hardness (~10 μm depth from surface) of plasma nitrided samples increases by 50% compared to that of the un-nitride substrate material irrespective of plasma gas composition. Surface hardening induced by nitriding, can be attributed to the [30]; i) solid solution strengthening induced due to the solution of nitrogen atoms in the iron lattice, ii) formation of fine precipitates of alloy nitrides which form as a consequence of matrix supersaturation from nitrogen that results in an additional strengthening via the dispersion-hardening mechanism and acting as barriers against movement of dislocations, and iii) development of compressive residual stress induced in diffusion layer as a result of some structural misfit because of formation of interstitial solid solution and alloying element nitrides.

From the hardness–depth profile, the case depth of nitrided samples is estimated to be 70, 90 and 105 μm for the $25N_2$, $50N_2$ and $75N_2$ flow rates, respectively. It can be seen that the case depth increases with increasing the nitrogen content in the plasma gas.

3.3. X-ray diffractograms

Fig. 3 shows typical X-ray diffraction patterns from un-nitrided and plasma nitrided samples at $25N_2$, $50N_2$ and $75N_2$ flow rates in the plasma gas composition. The diffraction pattern of un-nitrided M2 tool steel (Fig. 3a) shows two series of diffraction peaks, one series originating from the steel matrix and the other series from the dispersed carbide phases. Matrix peaks corresponds to the α-Fe (C, M)-martensite, where M refers to the different metallic alloying elements present in the steel composition. The identified carbide phases are

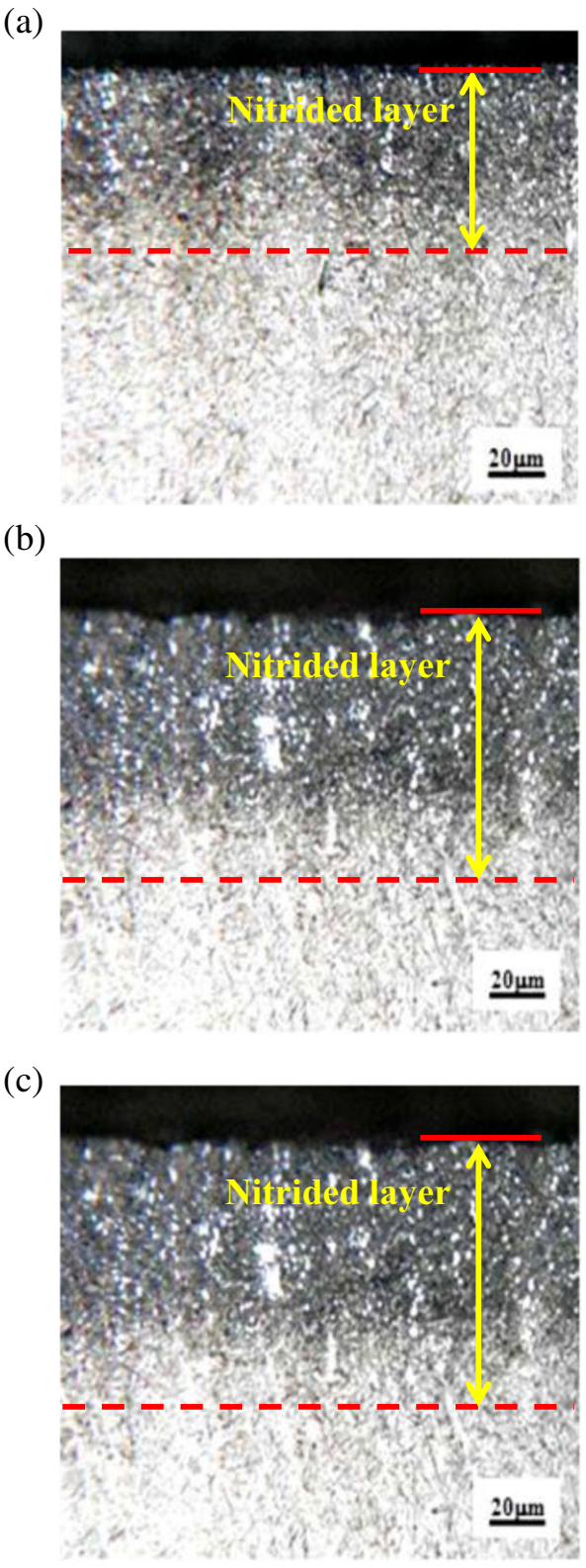

Fig. 1. Optical micrographs showing the cross-sectional microstructure of plasma nitrided specimens at different gas compositions: (a) 25 sccm N_2–75 sccm H_2, (b) 50 sccm N_2–50 sccm H_2, and (c) 75 sccm N_2–25 sccm H_2.

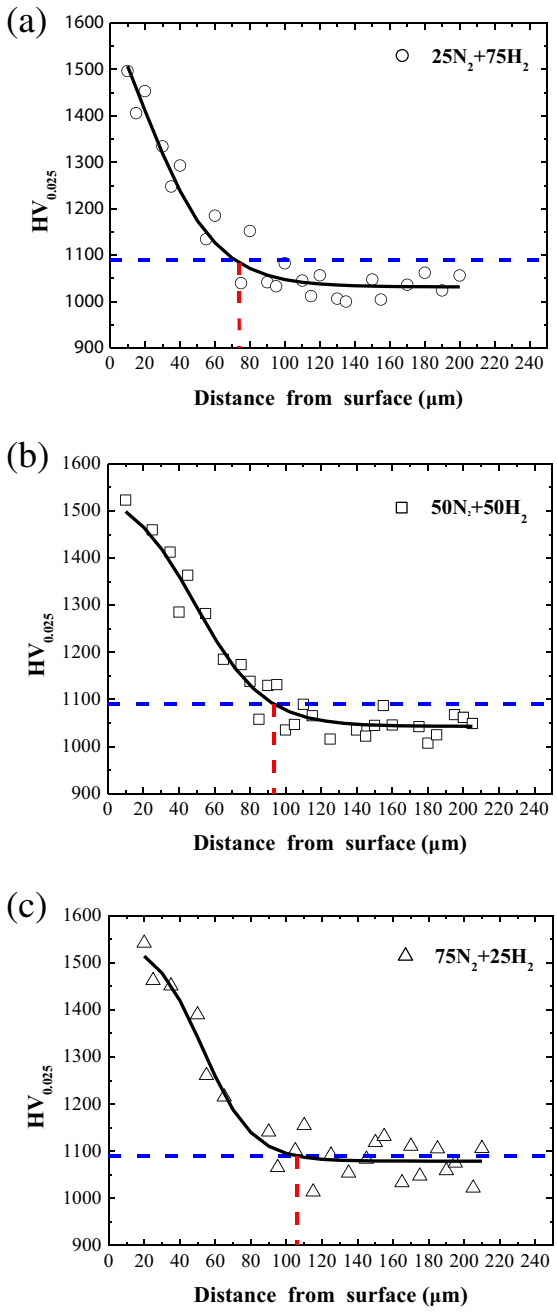

Fig. 2. Cross-sectional hardness-depth profiles after plasma nitriding at different gas compositions: (a) 25 sccm N_2–75 sccm H_2, (b) 50 sccm N_2–50 sccm H_2, and (c) 75 sccm N_2–25 sccm H_2.

either the VC or M_6C phases. In fact some of carbide forming elements like V, Cr, W and Mo may form their own simple carbides like VC or in combination with iron and other elements they form complex carbides like $(Fe,Cr)_3(W,Mo)_3C$.

The XRD pattern of samples plasma nitrided under a plasma gas flow rate of $25N_2$ (Fig. 3b) contains only a few peaks of the original phases. Instead, it contains a wide peak at $2\theta = 38.3°$ with very low intensity which could be attributed to the ε(110) peak. The absence of peaks from other iron nitrides (i.e. either $Fe_{2-3}N$ or Fe_4N nitride phases) indicates that the compound layer did not form at the $25N_2$ plasma gas flow. However, after plasma nitriding, there are considerable broadening and shifting of the (110) diffraction peak for α-Fe (C, M)-martensite.

On the other hand the X-ray diffractograms of plasma nitrided samples under plasma gas flow rates of $50N_2$ (Fig. 3c), and $75N_2$ (Fig. 3d) confirm the formation of the mono-phase ε-$Fe_{2-3}N$ compound layer at the sample surface.

The chemical composition of substrate material, process parameters and sputtering rate seems to be responsible for the phase composition of the compound layer. Carbon content of the steel influences the phase composition of the compound layer. According to the Fe–N–C phase diagram at low carbon concentration at the cathode surface a γ′-Fe_4N mono phase compound layer is formed. It is well established [31] that in DCPN the sputtering is directly responsible for the decarburization process occurring during the plasma nitriding. If the plasma nitriding is performed at low sputtering rates a significant amount of ε-$Fe_{2-3}N$ phase is produced [31]. In the present study as the nitriding process performed in a floating potential, the energy of ions arriving to the sample surface were only about 15 eV [32]. Such low energies cannot generate sputtering; therefore, the formation of epsilon nitride rather than Fe_4N phase is favored by the presence of high carbon in steel [33].

3.4. Surface roughness

The quantitative data of the surface roughness of the samples plasma nitrided at different gas compositions is indicated in Fig. 4. Minimum roughening occurred at $25N_2$ gas mixture, while nitriding at $75N_2$ gas mixture resulted in the roughest surface. Increasing the nitrogen content in gas mixture increased the roughness of the surface.

3.5. Wear resistance

Typical profilometery images of wear tracks of un-nitrided and nitrided samples after plasma nitriding at different N_2–H_2 plasma gas flow is shown in Fig. 5. It can be seen that wear scar is much larger on un-nitrided steel compared to that on plasma nitrided samples. The net worn out material volume, V_w, of samples as a function of the nitrogen gas flow rate in the plasma gas composition is shown in Fig. 6. The results suggest that plasma nitriding treatment of M2 tool steel improves its wear resistance between 20 and 90% with respect to the un-nitrided state depending on the N_2 flow rate in plasma nitriding gas composition. Investigations of nitriding steels using DC plasma [34–36] have indicated that, the improvement of tribological properties is considered to be a result of the combined effects of the microstructure, the high surface hardness and the high compressive residual stress in the nitrided layer. The high surface hardness can resist the plastic deformation. The super-saturated nitrogen in nitrided layer can introduce high compressive residual stresses, which will tend to close the formed microcracks or impede their formation during wear. On the other hand, formation of a compound layer on the sample surface induces high initial wear rate due to the breakdown of compound layer and formation of hard and abrasive particles [38].

It can be seen from Fig. 6 that the net worn out material volume, V_w, increases by increasing nitrogen content in the plasma gas flow. Among the nitrided samples, the highest wear resistance was recorded to the samples nitrided using $25N_2$ gas mixture.

4. Discussion

The increase in surface roughness during ion nitriding may be caused by contribution of three distinct phenomena: i) surface roughening in part by different lattice expansion of grains of polycrystalline material with the inward nitrogen diffusion from the differential swelling of the grains and in part by volume difference between the alloy nitrides inside the diffusion zone and the matrix, ii) sputtering caused by the collision of energetic particles accelerated from plasma toward the surface, iii) redeposition of the sputtered material on the surface. As the nitriding process performed in a floating potential, the energy

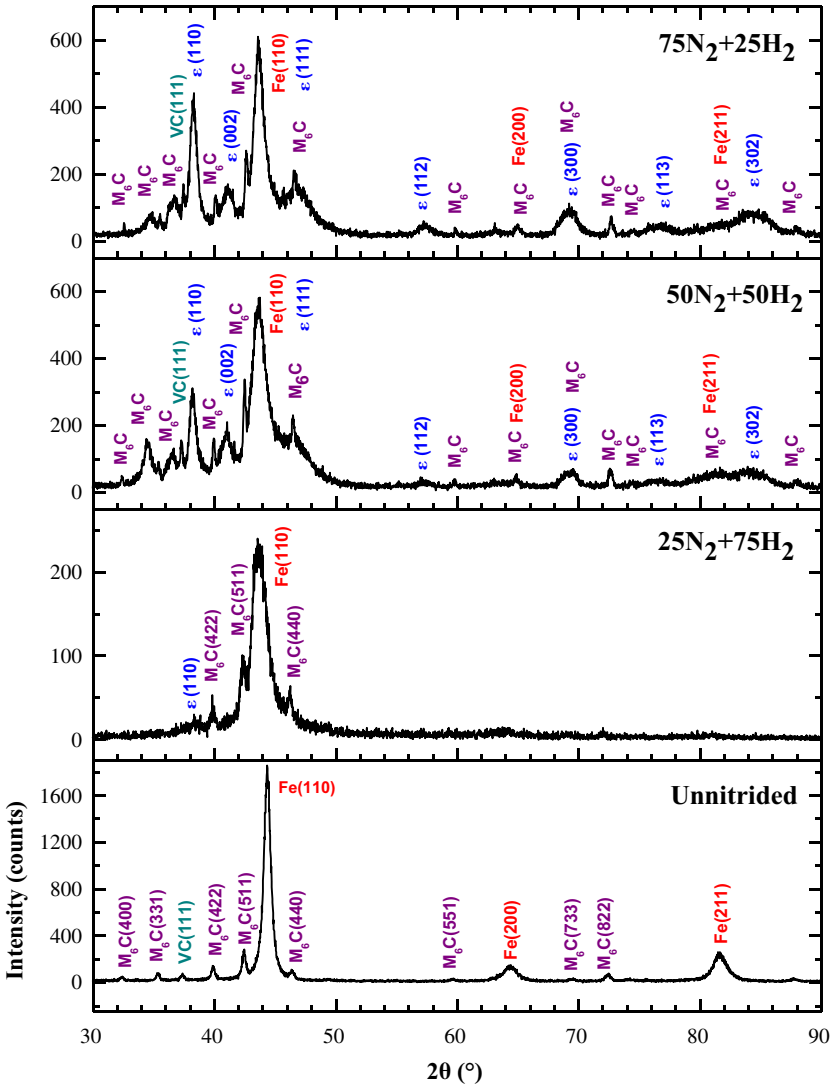

Fig. 3. X-ray diffractograms for the un-nitrided and plasma nitrided samples at the indicated N_2–H_2 gas composition ratios.

of ions arriving to the surface was only about 15 eV [32]. Such low energies cannot generate sputtering; therefore, the increase of surface roughness after nitriding can be entirely attributed to the volumetric lattice expansion associated to the nitrogen diffusion. Thus, inward diffusion of the higher nitrogen contents results in higher surface roughness. Having this discussion in mind one can conclude that, nitrided case depth increases with increasing nitrogen content in RF plasma gas composition under floating potential.

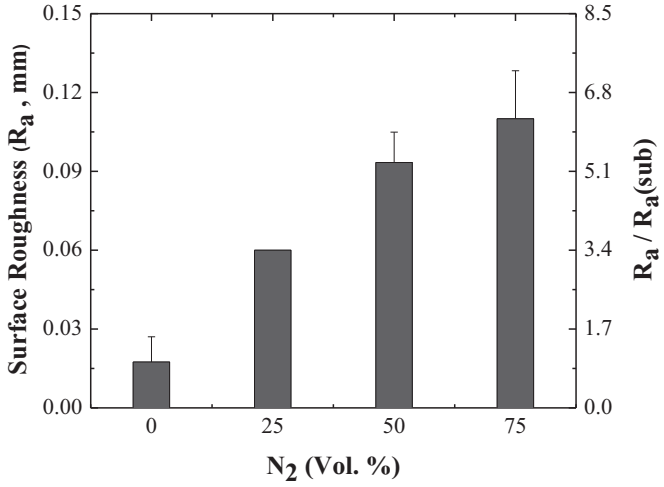

Fig. 4. Surface roughness (R_a, root mean square) results of AISI M2 tool steel before and after RF plasma nitriding at different gas compositions.

Evaluations of microhardness depth profiles, optical microscopy images and surface roughness data indicate that the thickness of nitrided layer increases with nitrogen content in the plasma gas. However, published data in DCPN shows that with increasing N_2:H_2 ratio in the plasma gas mixture the case depth decreases [15,37]. Increasing the amount of N_2 gas in DCPN processes requires a lower voltage to be applied. Due to the lower applied voltage, the amount of the ionized gases and the kinetic energy of the ions are decreased [38]. However, Gammer et al. [39] by fixing the bias voltage in DCPN of AISI D2 steel at a value of 450 V showed that diffusion zone depth increases up to a depth of 40 μm as the nitrogen contents rises up to 80%.

Similar to the analysis done by Corengia et al. [40], as the (110) peak of the ε-$Fe_{2-3}N$ phase has enough intensity and does not overlap with other substrate peaks, comparing its intensity for different samples reflects the amount of the ε-$Fe_{2-3}N$ phase on them in a semi-quantitative manner. The intensity of the ε(110) diffraction line increases by increasing nitrogen gas flow rate in the plasma gas composition. This indicates that the thickness of compound layer increases with increasing the amount of the N_2 in the N_2–H_2 plasma gas flow.

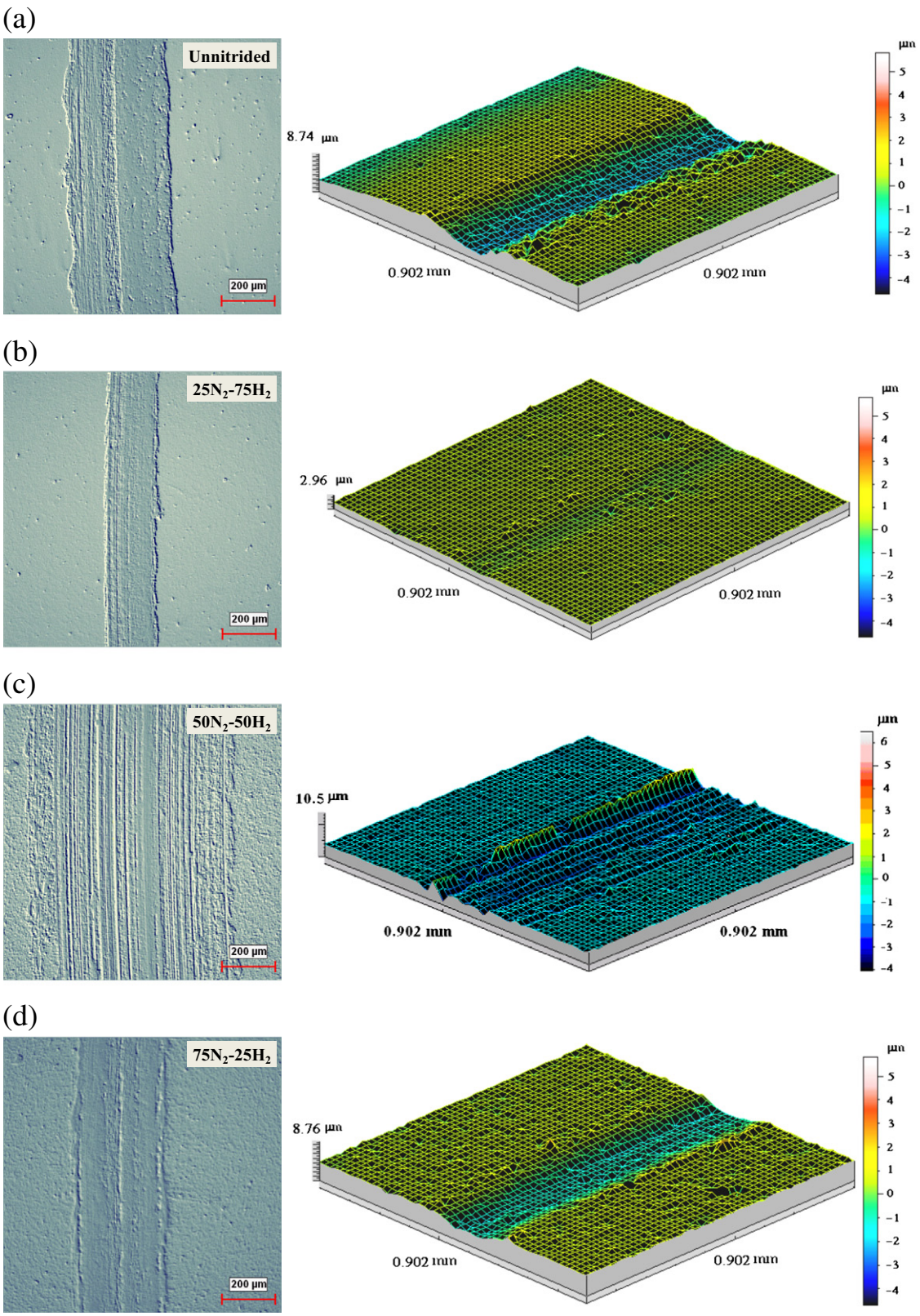

Fig. 5. Surface profiles of wear tracks (a) before nitriding and (b) after plasma nitriding at 25 sccm N_2–75 sccm H_2, (c) 50 sccm N_2–50 sccm H_2 and (d) 75 sccm N_2–25 sccm H_2.

This result is in close agreement with Alsaran et al. [15] report concerning the effect of the N_2 concentration in the N_2–H_2 plasma gas flow on the thickness of the compound layer. However, previous investigations in DC plasma nitriding of M2 tool steel demonstrated the absence of compound layer for samples nitrided with a 5 vol.% N_2–95% H_2 gas mixture [41–44], and the presence of the ε compound layer for the 25% N_2–75% H_2 [45] and 75% N_2–25% H_2 [41,42] plasma gas mixtures.

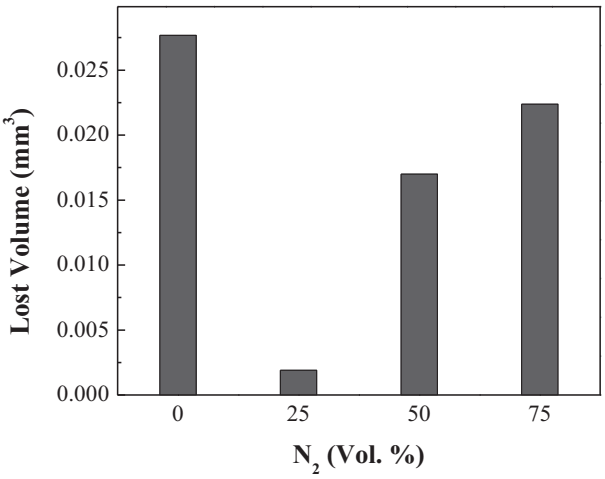

Fig. 6. Lost volume of M2 steel samples as a function of nitrogen content in the plasma gas.

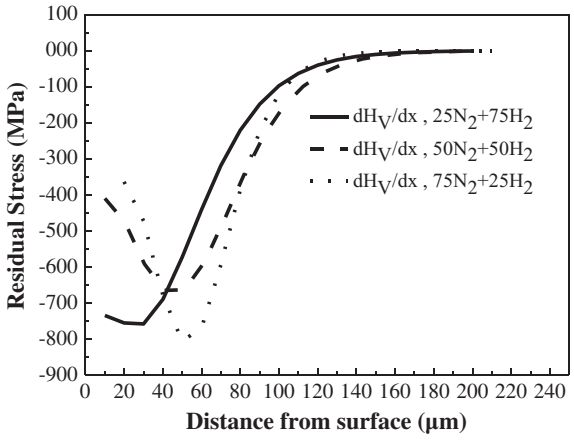

Fig. 7. In-depth residual stress distribution for M2 steel samples nitrided at different plasma gas compositions.

From the results of the XRD analysis one can conclude that for samples nitrided using the $25N_2$ gas mixture the thickness of the ε-$Fe_{2-3}N$ phase (compound layer) is negligible. On the other hand, the ε-$Fe_{2-3}N$ phase at the outer surface of the samples plasma-nitrided using the $50N_2$ and $75N_2$ gas mixtures has sufficient thickness to form a continuous thin layer. The ε-$Fe_{2-3}N$ phase is a brittle material and cannot withstand and support the high contact loads without cracking. Surface crack generated in the ε-$Fe_{2-3}N$ phase can easily grow and enter into the diffusion zone leading to faster wear of the nitride sample. Therefore, lower wear resistance of the M2 tool steel samples plasma nitrided using higher volume fraction of nitrogen in plasma gas flow may be attributed to the formation of the ε-$Fe_{2-3}N$ phase at the sample surface. This implies that for effective enhancement of wear resistance of the M2 tool steel by plasma nitriding it is essential to avoid formation of a compound layer by choosing appropriate plasma nitriding conditions. Rocha et al. [42] have also reported the lowest wear rate for sandblasted drills plasma-nitrided with 5 vol.% N_2–95 vol.% H_2 plasma gas without formation of a compound layer. They indicated the higher brittleness of samples nitrided with 76 vol.% N_2–24 vol.% H_2 plasma gas induced by grain boundary precipitation and the presence of tensile residual stresses in the compound layer which are possible reasons for the higher wear rates compared to surface treatments with 5 vol.% N_2. According to the recommendation given in the [46] the nitrided layers consisted of only diffusion zone improve the durability of M2 tool steel and the brittleness of the punch head can be avoided.

Residual stresses developed during nitriding or deposition of protective surface coatings have strong influences on the wear resistance and wear mechanism of the treated surfaces. Moderate levels of compressive residual stresses have beneficial effects on wear resistance. In order to predict the wear behavior of the nitride surface it is essential to know the sign and the magnitude of the residual stresses. However, the accurate and explicit measurement of the residual stress values in the plasma nitrided samples is not straightforward due to the stress gradient developed in the nitrided layer.

In order to evaluate residual stresses distribution across the nitrided layer more precisely, estimated values were obtained from modeling of the residual stresses as a function of a microhardness-related parameter; by deriving the measured microhardness depth profiles as a function of depth [47,48]. Microhardness depth profile derived over depth for plasma nitrided M2 tool steel for three different gas compositions is given in Fig. 7. It is seen that the residual stresses in the nitrided layer are compressive. The sign and relative magnitude of residual stress in the compound can also be estimated from shifting of the XRD peak. As shown in Table 1, in all the plasma nitrided samples the ε (110) peak shifts to smaller diffraction angles compared with the (110) peak position for an unconstrained ε ($2\theta_0$), indicating presence of compressive residual stress. The degree of ε (110) peak shifting toward small angles decreases with increasing N_2 flow rate in plasma gas due to the decreasing compressive stress. This confirms the results reported in Fig. 7.

According to Fig. 7 the maximum compressive stresses take place at a certain depth below the sample surface. It can be seen that compressive residual stresses in near surface for specimens nitrided with $25N_2$ are higher than those nitrided using $50N_2$ and $75N_2$ gas mixtures. High compressive residual stresses should have a beneficial effect by delaying crack initiation and growth. These results suggest that use of $25N_2$ gas mixture to obtain the right combination of nitride layer structure, thickness, hardness and wear resistance.

5. Conclusions

In the present work, AISI M2 tool steel samples were plasma nitrided using a RF plasma nitriding reactor operating under floating potential in a N_2–H_2 plasma gas flow and the effect of the N_2 flow rate on the microstructure and wear resistance of nitrided samples was investigated. Based on the obtained results the following conclusions can be drawn:

1- The nitrided layer thickness, determined using optical micrographs and microhardness profiles, increases by increasing nitrogen content in the plasma gas mixture.

2- XRD analysis showed that in the $25N_2$ plasma gas, the nitrided layer consists of mainly a diffusion zone. At the higher nitrogen contents of 50 and 75 sccm besides the diffusion zone, a ε-$Fe_{2-3}N$ iron nitride layer forms at the sample surface.

3- The surface hardness of samples increases significantly after nitriding. The hardness of the nitrided layer was determined to be about $1600HV_{0.025}$, close to the surface, irrespective of gas composition.

4- Compared with hardening by quench and tempering, plasma nitriding improves the wear resistance of the AISI M2 high speed tool steel. The maximum wear resistance for quench-tempered AISI

Table 1
Diffraction line position of the ε (110) peak at different gas compositions.

Sample	2θ-ε (110)	θ	d	$d-d_0$	$2\theta-2\theta_0$
$25N_2$	–	–	–	–	–
$50N_2$	38.2107	19.1053	2.3534	0.0194	−0.3293
$75N_2$	38.2805	19.1402	2.3493	0.0153	−0.2595
$d_0 = 2.33400$, $2\theta_0 = 38.54$					